

Quantum phases in a doped Mott insulator on the Shastry-Sutherland lattice

Jun Liu,¹ Nandini Trivedi,² Yongbin Lee,¹ B. N. Harmon,¹ and Jörg Schmalian¹

¹Department of Physics and Astronomy and Ames Laboratory, Iowa State University, Ames, Iowa 50011, USA

²Department of Physics, Ohio State University, Columbus, Ohio 43210, USA

(Dated: May 17, 2018)

We propose the projected BCS wave function as the ground state for the doped Mott insulator $\text{SrCu}_2(\text{BO}_3)_2$ on the Shastry-Sutherland lattice. At half filling this wave function yields the exact ground state. Adding mobile charge carriers, we find a strong asymmetry between electron and hole doping. Upon electron doping an unusual metal with strong valence bond correlations forms. Hole doped systems are d -wave RVB superconductors in which superconductivity is strongly enhanced by the emergence of inhomogeneous plaquette boi

The physics of doped Mott insulators is at the heart of some of the most interesting and challenging problems in condensed matter physics[1]. In the extreme “atomic” limit, the localization of electrons in the Mott insulating state leads to a macroscopic degeneracy of their spin or orbital degrees of freedom. Lifting this degeneracy via non-local quantum fluctuations gives rise to the rich variety of competing ground states in real materials. In many cases magnetic or orbital order prevails. In systems with geometric frustration and strong quantum fluctuations the possibility of a ground state without such order exists. Strong quantum mechanical fluctuations are also believed to induce unconventional superconductivity in doped Mott insulators and are related to the emergence of resonating valence bond (RVB) type fluctuations[2]. The investigation of doped Mott insulators without long range magnetic order at half filling is therefore the most direct way to uncover the nature of the strong local quantum fluctuations and their impact on the charge carrier dynamics, including superconductivity. It allows one to address questions such as: *Are all doped RVB states superconductors?* *What is the role of spatial inhomogeneities?* or *What determines the stability of states such as the d -wave resonating valence bond?*. By analyzing a specific example, doped $\text{SrCu}_2(\text{BO}_3)_2$ with Cu-spins on a Shastry-Sutherland lattice, we give answers to these interesting questions.

$\text{SrCu}_2(\text{BO}_3)_2$ is a Mott insulator with a low temperature spin gap $\Delta_s \simeq 30\text{K}$ [3, 4]. The Cu^{2+} states with $s = \frac{1}{2}$ spins interact predominantly within two dimensional CuBO_3 -planes and form dimers along the bond with dominant spin-spin interaction. The topology of the Cu-sublattice is shown in Fig. 1. The dominant, intra-dimer exchange interaction J' is along the diagonal bonds, while the smaller inter-dimer exchange J is along the x - and y -axes. There are two remarkable aspects of this material. First, the exact ground state of the Heisenberg model, on the lattice shown in Fig. 1 was obtained by Shastry and Sutherland[5]. For sufficiently large J' the exact ground state energy per site is $E_0/N = -\frac{3}{8}J'$. The ground state wave function is an orthogonal dimer state $|\Phi_{\text{od}}\rangle$, i.e. a direct product of singlets along the bonds

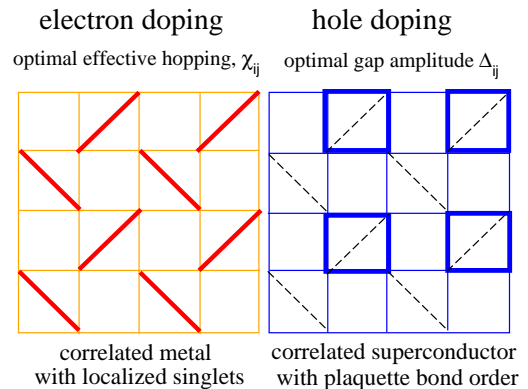


FIG. 1: Shastry Sutherland lattice with effective hopping χ_{ij} (for electron doping) and local pairing strength Δ_{ij} (for hole doping). The width of each line determines the magnitude χ_{ij} or Δ_{ij} , respectively. For electron doping, strong correlations along the diagonals occur, reminiscent of the undoped valence bond crystal. For hole doping, the nature of the pairing state changes, leading to d -wave superconductivity and an inhomogeneous plaquette pattern of the bond strength. Plaquette states with large Δ_{ij} around the two different diagonal orientations are degenerate.

connected by J' : $|\Phi_{\text{od}}\rangle = \prod_{\langle ij \rangle} (|\uparrow\downarrow\rangle_{ij} - |\downarrow\uparrow\rangle_{ij}) / \sqrt{2}$. Shastry and Sutherland demonstrated that this is the ground state for $J'/J > 2$. More recent numerical results[6, 7, 8, 9, 10, 11] support a transition for J'/J between 1.42 and 1.47. In the state $|\Phi_{\text{od}}\rangle$ singlets are localized, making this Mott insulator a valence bond crystal without long range magnetic order. The second interesting aspect of $\text{SrCu}_2(\text{BO}_3)_2$ is that $J'/J \simeq 1.57$ ($J' \simeq 85\text{K}$ and $J \simeq 54\text{K}$ [4]) is close to the regime where $|\Phi_{\text{od}}\rangle$ ceases to be the ground state. The valence bond crystal is comparatively fragile and competing states become relevant. Interesting proposals for competing phases at half filling include helical ordered states[12, 13], plaquette singlet states[8, 11, 13] and a deconfined spinon phase[13].

In this paper we investigate the stability of the valence bond crystal, and the emergence of superconductivity, flux phases and inhomogeneous states in doped

$\text{SrCu}_2(\text{BO}_3)_2$. We use a resonating valence bond variational wave function[2] that includes the *exact* ground state energy for the half filled parent compound, making the approach particularly well controlled for small doping. We demonstrate that upon adding charge carriers, the system displays a *strong asymmetry* between electron and hole doping. For electron doping a non-superconducting but metallic phase with strong valence bond correlations forms, while an unconventional superconductor emerges for hole doping. In the latter case a spontaneous breaking of the spatial symmetry occurs, where the paring gap forms a plaquette pattern, while the charge density remains uniform (see Fig. 1). We then show that for hole doping superconductivity of this inhomogeneous state is *strongly enhanced* compared to the homogeneous state.

In order to describe doped $\text{SrCu}_2(\text{BO}_3)_2$ we start from the t - J model[14]:

$$H = \sum_{ij,\sigma} t_{ij} \tilde{c}_{i\sigma}^\dagger \tilde{c}_{j\sigma} + \sum_{i,j} J_{ij} \left(\mathbf{S}_i \cdot \mathbf{S}_j - \frac{1}{4} n_i n_j \right), \quad (1)$$

where $\sum_{\sigma} \tilde{c}_{i\sigma}^\dagger \tilde{c}_{i\sigma} \leq 1$, the tilde indicates that these operate in the projected Hilbert space, and the remaining notation is standard. In addition to Eq.1 we also include three site hopping terms[15] (not shown explicitly) that are of same order in t/U and become relevant for larger doping. We include hopping elements t and t' for the bonds with exchange interaction J and J' , respectively.

Hole doping in the t - J model is achieved by taking out electrons. To describe electron doping we perform a particle-hole transformation and take out holes. This transformation changes the sign of t' but not of t . Thus, one sign of t' corresponds to hole, the other sign to electron doping. Since t' is the largest hopping element we expect an asymmetry between electron and hole doping. The effect is already visible if one analyses the single hole state on a 4-site lattice. A doped carrier is localized on the diagonals for $t' < 0$ and delocalizes for $t' > 0$. Experiments so far determine $J'/J = (t'/t)^2$ but not the sign of t' .

In order to determine the crucial sign of the diagonal hopping elements t' we perform electronic structure calculations for $\text{SrCu}_2(\text{BO}_3)_2$. In cuprate superconductors such calculations give the proper Fermi surface and band dispersion[16] despite their problems with the Mott insulating state and mass renormalization effects. We assume the same is true in our case. In Fig. 2 we show our results in comparison with a tight binding model where we ignore correlation effects, making the system a (semi)metal instead of a Mott insulator. In the LDA calculation we ignore magnetic order. Except for the detailed behavior around the M -point the tight binding model gives a very reasonable description of the electronic structure. It also demonstrates that other bands, not included in the tight binding approach, are well separated in en-

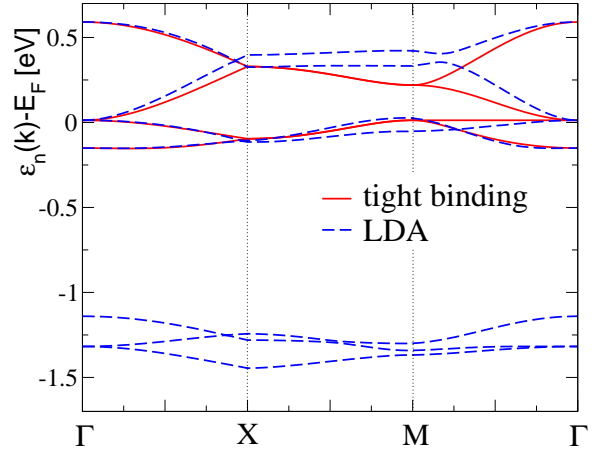


FIG. 2: Bandstructure of $\text{SrCu}_2(\text{BO}_3)_2$ obtained using density functional theory in comparison with a tight binding fit. Only the in-plane dispersion of the bands is shown. The bands close to E_F are made of $\text{Cu}-3d_{x^2-y^2}$ and $\text{O}-2p$ states, while the well separated bands around -1.25eV consist of $\text{O}-2p$ and $\text{Cu}-3d_{xz}$ and $3d_{yz}$ states.

ergy. A fit close to the Γ -point yields $t = 0.09\text{eV}$ and $t' = 0.104\text{eV} > 0$. The ratio $t'/t \simeq 1.15$ is slightly smaller than the value 1.25, obtained from the ratio of the exchange constants. However, a fit where one forces $t'/t = 1.25$ still gives a very good description of the LDA band-structure. In what follows we measure energies in units of t , use $t' = \pm 1.25t$ for hole and electron doping and $J_{ij} = 0.3|t_{ij}|$. The qualitative behavior of our results is unchanged if we use the experimental values for J_{ij} and the unrenormalized values for t_{ij} listed above.

We now include the effects of strong correlation into the calculation by using a resonating valence bond ground state wave function[2, 15, 17, 18]

$$|\Psi\rangle = P |\Phi_{\text{BCS}}\rangle, \quad (2)$$

where P projects out all doubly occupied states. $|\Phi_{\text{BCS}}\rangle$ is the BCS-ground state wave function. The RVB description is particularly appealing as it reproduces the exact ground state at half filling (see below). $|\Phi_{\text{BCS}}\rangle$ is the fixed particle projection of the ground state of

$$H_{\text{BCS}} = \sum_{i,j,\sigma} \chi_{ij} c_{i\sigma}^\dagger c_{j\sigma} + \sum_{ij} \left(\Delta_{ij} c_{i\uparrow}^\dagger c_{j\downarrow}^\dagger + h.c. \right). \quad (3)$$

The effective hopping elements χ_{ij} and pairing gaps Δ_{ij} are the variational parameters of our many body wave function and are determined by minimizing the energy $E = \langle \Psi | H | \Psi \rangle / \langle \Psi | \Psi \rangle$. E is evaluated using the Monte Carlo approach of Ref.19 for 12×12 up to 18×18 lattices. The many body wave function Eq.2 also allows determination of the long range correlations between pairs, enabling us to distinguish between local pairing and off diagonal long range order (ODLRO). Only the latter corresponds to superconductivity, yields a Meissner effect

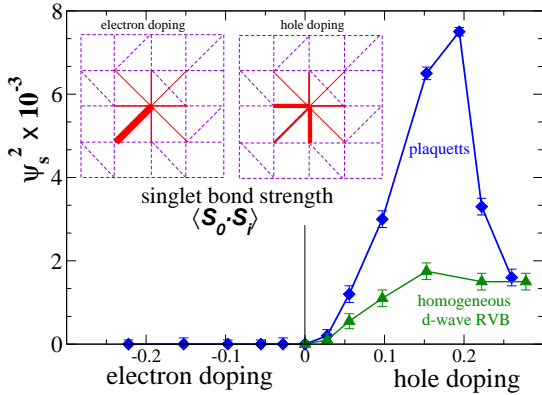


FIG. 3: Superconducting order parameter, signaling ODLR for hole doped systems. Even though the wave function for electron doped systems is characterized by a pairing strength $\Delta_{ij} \neq 0$ in the BCS wave function, no superconducting order exists. From the analysis of the low energy Drude weight we conclude that the system is a metal. For hole doped systems d -wave superconductivity emerges. The superconducting order parameter is strongly enhanced in the inhomogeneous plaquette phase. The inset shows the local spin correlations for electron and hole doping. The thickness of the line refers to the magnitude of $\langle \mathbf{S}_0 \cdot \mathbf{S}_j \rangle$. All nearest and next nearest neighbor correlations are antiferromagnetic.

and flux quantization. To this end we analyze the pairing correlation function, $F_{\mathbf{a},\mathbf{b}}(\mathbf{r} - \mathbf{r}') = \langle \Psi | b_{\mathbf{r},\mathbf{a}}^\dagger b_{\mathbf{r}',\mathbf{b}} | \Psi \rangle$, with $b_{\mathbf{r},\mathbf{a}} = \frac{1}{2}(c_{\mathbf{r}+\mathbf{a},\downarrow}c_{\mathbf{r}\uparrow} - c_{\mathbf{r}+\mathbf{a},\uparrow}c_{\mathbf{r},\downarrow})$ and \mathbf{a}, \mathbf{b} nearest neighbor vectors. $|\psi_s|^2 \propto F_{\mathbf{a},\mathbf{b}}(\mathbf{R} = \mathbf{r} - \mathbf{r}' \rightarrow \infty)$ determines the superconducting order parameter ψ_s .

Undoped system: At half filling, the variational wave function in Eq.2 yields the exactly known ground state energy E_0 with an accuracy 10^{-7} . We further obtain the expected spin correlations $\langle \mathbf{S}_i \cdot \mathbf{S}_j \rangle$ which equals $-\frac{3}{4}$ for sites i and j on the same dimer bond and vanishes otherwise with error bars of 10^{-4} . Thus, at half filling the RVB wave function, Eq.2, reproduces the exact ground state of the Shastry-Sutherland model, making it an ideal starting point to investigate doped systems.

Doped valence bond crystal: At finite electron doping, we find that the renormalized diagonal hopping χ' that enters $|\Phi_{\text{BCS}}\rangle$ as a variational parameter is significantly enhanced compared to the bare values. For doping values $x \simeq 0.1$ we find $\chi'/\chi \simeq 1.5t'/t$, see also the left panel of Fig. 1. The spin correlations $\langle \mathbf{S}_i \cdot \mathbf{S}_j \rangle$ shown in the inset of Fig. 3, are large for sites i and j on the same diagonal bond and very small otherwise and mimic the behavior of the orthogonal dimer state of the undoped parent compound.

The pairing gap Δ_{ij} is finite (for example, at electron doping $x = 0.1$, we obtain the gaps along diagonal bonds $\Delta_{i,i+x\pm y} \approx 0.3t$). It is remarkable that this many body state with finite local pairing gap does not show any indication for off diagonal long range order (see Fig. 3). The pairing correlation function $F_{\mathbf{a},\mathbf{b}}(\mathbf{R})$ rapidly vanishes be-

yond the nearest neighbor. We also determined the low energy contribution of the Drude weight[15] and found $D_{\text{Drude}} \simeq 3.18xt$ for small x . Despite the addition of mobile charge carriers, singlets form on diagonal bonds and the system remains in a non-superconducting but metallic phase with strong valence bond correlations. The absence of superconductivity for $t' > 0$ is consistent with the finding of Ref.[20].

Correlated Superconductor: The hole doped case, on the other hand, shows superconductivity (see Fig.3). The pairing gap has $d_{x^2-y^2}$ symmetry with $\Delta_{i,i+\mathbf{x}} = -\Delta_{i,i+\mathbf{y}}$. Also its magnitude is larger for hole doping compared to the electron doped case (we find $\Delta_{i,i+\mathbf{x}} \simeq t$ for hole doping $x = 0.1$). The magnetic correlations in this superconductor are very different from the valence bond crystal. As shown in the inset of Fig. 3, we find $\langle \mathbf{S}_i \cdot \mathbf{S}_j \rangle < 0$ with rather comparable magnitude for *all* neighbors, even when they are coupled via the exchange interaction J .

As pointed out above, the origin for the strong asymmetry between hole and electron doping is due to the constructive ($t' > 0$) and destructive ($t' < 0$) interference of hopping paths in the system. This leads to a delocalization of singlets and a true RVB state for hole doping while for electron doping the underlying valence bond crystal is only moderately affected.

Inhomogeneous Superconductor: So far we assumed that the system is fully homogeneous, i.e. that no spatial symmetry in the problem is broken. Next we allow for the local potentials χ_{ii} , effective hopping elements χ_{ij} as well as pairing gaps Δ_{ij} to vary in space. Specifically, we allow for arbitrary values of these quantities inside the crystallographic unit cell, consisting of four Cu-sites. For electron doping no additional symmetry is broken. In case of hole doping, we find that the spontaneous emergence of inhomogeneous solutions leads to a reduction of the ground state energy ($\Delta E \simeq 4.3 \times 10^{-3}t$ for $x = 0.1$ which is three times the energy gain of the homogeneous d -wave state compared to the $\Delta_{ij} = 0$ state). While the charge is homogeneous, we find large variations of the pairing gaps following the pattern indicated in the right panel of Fig.1. For $x \simeq 0.1$ we find for strong bonds a gap amplitude $\Delta \simeq 2.3t$ compared to $\simeq 0.2t$ for weak bonds. The plaquette state with periodic variation of the pairing strength is driven by a gain in the kinetic energy.

In this plaquette state, the effective hybridizations χ' on the diagonals also varies in space. χ' on diagonals surrounded by large pairing gaps is reduced compared to χ' on plaquettes with small gaps. At half filling, an analysis of the Shastry-Sutherland lattice with $\text{Sp}(N)$ symmetry[13] led to several plaquette states, including one similar to ours, once strong quantum fluctuations were taken into account. Doping with charge carriers is clearly one route to enhance quantum fluctuations. Physically, d -wave RVB fluctuations between the states $| \rangle$ and $| \langle \rangle$ inside a plaquette seem strongest if the system is allowed to break up in a spatially inhomogeneous pat-

tern.

The most interesting aspect of this new plaquette ordered state is that long range superconducting order ψ_s is strongly enhanced in the plaquette state compared to the homogeneous state as seen in Fig. 3. The pairing correlation function $F_{\mathbf{a},\mathbf{b}}(\mathbf{R})$ reaches its long distant limit after several lattice constants. Strong pairing in plaquettes separated by less than this superconducting coherence length is therefore very efficient to boost a superconducting state[21]. For hole doping the magnitude $|\psi_s|^2$ is approximately 10% of the value one obtains within BCS-theory for the same pairing gap. For electron doping the effect of quantum fluctuations much more dramatic since $|\psi_s|^2 = 0$ even though a BCS theory with finite gap would always yield a finite order parameter.

A simple analytic approach that provides useful insight in case of other doped Mott insulators is the slave boson mean field theory. The approach is closely related to the wave function, Eq.2, with the key difference that the projection P is done only on the average. Performing a slave boson calculation, we find, in agreement with earlier work[14], that the strong asymmetry between electron and hole doping does not emerge. The plaquette state found in this paper does not follow from the slave boson calculation either. Finally, by using the full projection we searched unsuccessfully for a staggered flux phase with $\chi_{ij} = \chi e^{\pm i\theta}$, found in a slave bosons calculation[22]. These results demonstrate that proper projection, which enters the slave boson theory via strong gauge field fluctuations, is crucial for the Shastry-Sutherland lattice.

In summary, we have identified a doped Mott insulator with a very rich behavior as function of varying charge carrier concentration. Electron doped systems display metallic phases with strong valence bond correlations and are the first example for a doped Mott insulator where an RVB-wave function yields local pairing but no superconductivity. Hole doped systems enter a d-wave RVB state, become superconducting and an inhomogeneous bond order emerges spontaneously which enhances superconductivity. From the energy gain of the paired state and the values of the exchange energies J_{ij} we estimate a superconducting transition temperature T_c of several Kelvin. Experimentally, attempts to dope $\text{SrCu}_2(\text{BO}_3)_2$ have not led to metallic behavior[23]. However, recent advances in the sample preparation of transition metal oxides[24] give us every reason to be optimistic that the obstacles to dope this material can be overcome. We hope that our results stimulate research in this direction.

We are grateful to David C. Johnston who initially encouraged us to investigate this problem. In addition we are grateful to I. Affleck, C. Batista and M. Randeria for helpful discussions. This research was supported by the Ames Laboratory, operated for the U.S. Department of

Energy by Iowa State University under Contract No. DE-AC02-07CH11358 and by a Fellowship from the Institute for Complex Adaptive Matter (JL). We acknowledge the use of computational facilities at the Ames Laboratory.

- [1] J. Zaanen, S. Chakravarty, T. Senthil, P. W. Anderson, P. A. Lee , J. Schmalian, M. Imada, D. Pines, M. Randeria, C. Varma, M. Vojta, T. M. Rice, *Nature Physics* **2** , 138 (2006).
- [2] P. W. Anderson, *Science* **235**, 1196 (1987).
- [3] H. Kageyama, K. Yoshimura, R. Stern, N. V. Marshnikov, K. Onizuka, M. Kato, K. Kosuge, C. P. Slichter, T. Goto, and Y. Ueda, *Phys. Rev. Lett.* **82**, 3168 (1999).
- [4] For a recent review, see: S. Miyahara and K. Ueda, *J. Phys.: Condens. Matter* **15**, R327 (2003).
- [5] B. S. Shastry and B. Sutherland, *Physica B* **108**, 1069 (1981).
- [6] S. Miyahara and K. Ueda, *Phys. Rev. Lett.* **82**, 3701 (1999).
- [7] Z. Weihong, C. J. Hammer, J. Oitmaa, *Phys Rev. B* **60**, 6608 (1999).
- [8] A. Koga and N. Kawakami, *Phys. Rev. Lett.* **84**, 4461 (2000).
- [9] E. Müller-Hartmann, R. R. P. Singh, C. Knetter and G. S. Uhrig, *Phys. Rev. Lett.* **84**, 1808 (2000).
- [10] Z. Weihong, J. Oitmaa, and C. J. Hammer, *Phys. Rev. B* **65**, 014408 (2002).
- [11] A. Läuchli, S. Wessel, and M. Sigrist, *Phys. Rev. B* **66**, 014401 (2002).
- [12] M. Albrecht and F. Mila, *Europhys. Lett.* **34**, 145 (1996).
- [13] C. H. Chung, J. B. Marston, and S. Sachdev, *Phys. Rev. B* **64**, 134407 (2001).
- [14] B.S. Shastry and B. Kumar, *Prog. Theor. Phys. Suppl.* **145**, 1 (2002).
- [15] A. Paramekanti, M. Randeria, N. Trivedi, *Phys. Rev. Lett.* **87**, 217002 (2001); *ibid* *Phys. Rev. B* **70**, 054504 (2004).
- [16] W. E. Pickett, *Rev. Mod. Phys.* **61**, 433 (1989).
- [17] C. Gross, R. Joynt, and T. M. Rice, *Z. Phys. B* **68**, 425 (1987); C. Gros, *Phys. Rev. B* **38**, 931 (1988).
- [18] P. W. Anderson, P. A. Lee, M. Randeria, T. M. Rice, N. Trivedi, F. C. Zhang, *J. Phys. Cond. Mat.* **16** R755 (2004).
- [19] D. M. Ceperley, G. V. Chester, M. H. Kalos, *Phys. Rev. B* **16**, 3081 (1977).
- [20] P. W. Leung and Y. F. Cheng, *Phys. Rev. B* **69**, 180403 (2004).
- [21] I. Martin, D. Podolsky and S. A. Kivelson, *Phys. Rev. B* **72**, 060502(R) (2005).
- [22] C.-H. Chung and Y. B. Kim, *Phys. Rev. Lett.* **93**, 207004 (2004).
- [23] G. T. Liu, J. L. Luo, N. L. Wang, X. N. Jing, D. Jin, T. Xiang, and Z. H. Wu, *Phys. Rev. B* **71**, 014441 (2005).
- [24] Y. Kohsaka, M. Azuma, I. Yamada, T. Sasagawa, T. Hanaguri, M. Takano, and H. Takagi, *Journ. of the Amer. Chem. Soc.* **124**, 12275 (2002).